# THE EFFECT OF HORIZONTAL GRADIENTS OF HEIGHT-FIELD FORECAST ERROR VARIANCES UPON OI FORECAST ERROR STATISTICS

OFFICE NOTE 296

STEPHEN E. COHN*

COURANT INSTITUTE OF MATHEMATICAL SCIENCES

NEW YORK UNIVERSITY

NEW YORK, N.Y. 10012

and

LAUREN L. MORONE

DEVELOPMENT DIVISION

OCTOBER 1984



---

* Supported in part by NOAA Grant No. NA84AA-D-00018

# The Effect of Horizontal Gradients of Height-Field Forecast Error Variances Upon OI Forecast Error Statistics

## Contents

## Abstract

In the formulation of statistical relationships among forecast errors in the optimal interpolation (OI) analysis system at NMC, it is currently assumed that horizontal gradients of the height-field forecast error standard deviation, $\sigma^z$, are negligible. This homogeneity assumption is reasonable only in areas of uniform data density and quality. The dominant feature on the maps of $\sigma^z$ actually produced by the OI system is in fact the rapid change of $\sigma^z$ near boundaries between data-dense and data-sparse regions.

In this note we rederive the statistical relationships among forecast errors, without assuming that the $\sigma^z$ field is homogeneous. The resulting forecast error statistics are compared with the conventional ones, using realistic $\sigma^z$ fields. The comparison shows that the wind-field forecast error standard deviations are increased over the entire globe, and by as much as about 30% in some regions. The wind-height and wind-wind forecast error correlations are changed even more dramatically. For example, the correlation between height and zonal wind forecast errors at a point is 0.0 if $\sigma^z$ is constant there, but becomes as large as about $\pm$ 0.6 at points where $\sigma^z$ is changing rapidly. More generally, the wind-height and wind-wind forecast error correlations lose the homogeneity and isotropy properties they possess in conventional OI formulations, in a manner reflecting the variability of data density and quality encountered over the globe.

## I. Introduction

A primary consideration in optimum interpolation (OI) analysis schemes is the specification of the forecast error covariance fields. At NMC, the auto-correlation of the height-field forecast error is modeled by an analytically prescribed function, and the covariances among the other variables are derived from it by assuming a geostrophic relationship among forecast errors (Bergman, 1979; McPherson et al., 1979). Another assumption made in the process of deriving the forecast error covariances is that the standard deviation $\sigma^z$ of the height-field forecast error is locally homogeneous. This means that at each analysis point, $\sigma^z$ is assumed constant over a two-dimensional area corresponding to the influence region of the correlation function, at NMC a circle with a radius of approximately 1500 km.

The homogeneity assumption is made in most, if not all operational multivariate OI analysis schemes (Bergman, 1979; Lorenc, 1982; Rutherford, 1976; Schlatter, 1975). However, it is a reasonable assumption only in areas of uniform data quality and availability. At boundaries between such areas, $\sigma^z$ changes quite rapidly over distances much less than 1500 km. In fact, the dominant feature on maps of forecast error standard deviations is precisely the presence of sharp gradients due to variable data density and quality (see Fig. 1).

It is a simple process mathematically to remove the homogeneity assumption from the OI forecast error covariance relationships. A few additional terms involving the east-west and north-south derivatives of $\sigma^z$ must be calculated. This increased computation time is one reason the homogeneity assumption was originally made. The recent acquisition of a CYBER 205 at NMC, in part, has prompted us to reconsider the homogeneity assumption.

We show in this paper that inclusion of the effect of horizontal gradients of $\sigma^z$ in the OI formulation alters significantly the wind-height and wind-wind forecast error covariances. The effect always increases the wind-field forecast error standard deviations, by up to about 30% in some regions. The wind-height and wind-wind correlations are altered even more dramatically. In particular, these correlations lose the homogeneity and isotropy properties they possess in conventional OI formulations, in a manner reflecting the variability of data density and quality encountered over the globe. In fact, these correlations all asymptote to the height-height correlation as logarithmic gradients of $\sigma^z$ increase. We show that this asymptotic effect is quite large near data-dense/data-sparse boundaries encountered in several regions of the world.

The relationships among forecast error covariances, variances, and correlations, including the effect of gradients of $\sigma^z$, are derived in Section II. These relationships are derived under the sole assumption that forecast errors are geostrophic. No particular form is assumed for the height-height correlation field. Section III discusses implementation details, as well as drawbacks and generalizations of the geostrophic assumption. The magnitude of the effect of gradients of $\sigma^z$ upon forecast error standard deviations and correlations is discussed in Section IV. Correlation function plots using simulated fields are presented in Section V. These plots are based on a height-height forecast error correlation model which is a Gaussian function of spherical distance. A companion paper (Morone and Cohn, 1984) details the effect of using various approximations to the spherical distance. Conclusions appear in Section VI.

## II. Derivation of OI Statistical Relationships

We derive in this section the general relationships among forecast error covariances, variances, and correlations, under the sole assumption that forecast errors are geostrophic, and given an arbitrary height-height forecast error covariance field. The main difference between our derivation and more conventional ones is that we account for the effect of horizontal gradients of height-height forecast error variances. Also, by leaving the height-height forecast error covariance arbitrary for now, it will be easy to derive in the companion paper the statistical relationships resulting from various formulations of the height-height forecast error covariance field.

To begin, let

$$u_i, \ v_i, \text{ and } z_i$$

denote the forecast errors in the zonal wind, meridional wind and height, at a point

$$P_i = ( \lambda_i , \ \Phi_i , \ p_i \ ),$$

where $\lambda$ , $\Phi$ and $p$ denote longitude, latitude and pressure. An overbar will denote the expectation, or ensemble average, so that

$$q_i' \equiv q_i - \overline{q_i} \ , \text{ where } q = u, \text{ v or } z,$$

denotes the departure of $q_i$ from its mean $\overline{q_i}$. The quantity

$$\overline{q_i' \ r_j'}, \text{ where } q = u, \text{ v or } z, \text{ and } r = u, \text{ v or } z,$$

is the covariance between $q_i = q( \lambda_i , \ \Phi_i , \ p_i \ )$ and $r_j = r( \lambda_j , \Phi_j , p_j )$. The standard deviations $\sigma_i^q$ are the positive square roots of the variances

$$( \sigma_i^q )^2 = \overline{q_i' \ q_i'}.$$

The correlations $C_{ij}^{qr}$ between $q_i$ and $r_j$ are defined by

$$C_{ij}^{qr} \equiv \overline{q_i' \ r_j'} \Big/ \sigma_i^q \ \sigma_j^r \ .$$

When i = 1 and j = 2, we drop the subscripts on $C_{ij}^{qr}$ , i.e., $C^{qr} = C_{12}^{qr} =$

$$C^{qr} \left( \lambda_1, \Phi_1, p_1; \lambda_2, \Phi_2, p_2 \right) .$$

The central assumption upon which OI statistical relationships are traditionally based is that forecast errors are geostrophic, with a relaxation of this assumption in the tropics:

$$u_i = \alpha_i \frac{\partial}{\partial \phi_i} z_i \quad , \quad v_i = \beta_i \frac{\partial}{\partial \lambda_i} z_i \quad , \tag{2.1a,b}$$

where

$$\alpha_i = -\frac{G_i g}{f_i a} \quad , \quad \beta_i = +\frac{G_i g}{f_i a \cos\phi_i} \tag{2.2a,b}$$

Here g is the acceleration due to gravity, a is the radius of the earth, $f_i = 2\Omega \sin\phi_i$ is the Coriolis parameter, and $G_i$ is the relaxation factor, or coefficient of geostrophy. We retain (2.1, 2.2) as our working assumption. Some implications, as well as some generalizations, of the geostrophic assumption itself are discussed in Section III.

Equations (2.1) immediately imply, in the usual way, that the height-height forecast error covariance field determines the remaining covariances. Taking expectations in each of (2.1a,b) we have

$$\overline{u_i} = \alpha_i \frac{\partial}{\partial \phi_i} \overline{z_i} \quad , \quad \overline{v_i} = \beta_i \frac{\partial}{\partial \lambda_i} \overline{z_i} \quad ; \tag{2.3a,b}$$

subtracting (2.3a,b) from (2.1a,b) gives

$$u_i' = \alpha_i \frac{\partial}{\partial \phi_i} z_i' \quad , \quad v_i' = \beta_i \frac{\partial}{\partial \lambda_i} z_i' \quad . \tag{2.4a,b}$$

From (2.4a,b) it then follows that

$$\overline{u_1' z_2'} = \alpha_1 \frac{\partial}{\partial \phi_1} \overline{z_1' z_2'} \quad , \quad \overline{z_1' u_2'} = \alpha_2 \frac{\partial}{\partial \phi_2} \overline{z_1' z_2'} \tag{2.5a,b}$$

$$\overline{v_1' z_2'} = \beta_1 \frac{\partial}{\partial \lambda_1} \overline{z_1' z_2'} \quad , \quad \overline{z_1' v_2'} = \beta_2 \frac{\partial}{\partial \lambda_2} \overline{z_1' z_2'} \tag{2.5c,d}$$

$$\overline{u_1' v_2'} = \alpha_1 \beta_2 \frac{\partial^2}{\partial \phi_1 \partial \lambda_2} \overline{z_1' z_2'} \quad , \quad \overline{v_1' u_2'} = \beta_1 \alpha_2 \frac{\partial^2}{\partial \lambda_1 \partial \phi_2} \overline{z_1' z_2'} \tag{2.5e,f}$$

$$\overline{u_1' u_2'} = \alpha_1 \alpha_2 \frac{\partial^2}{\partial \phi_1 \partial \phi_2} \overline{z_1' z_2'} \quad , \quad \overline{v_1' v_2'} = \beta_1 \beta_2 \frac{\partial^2}{\partial \lambda_1 \partial \lambda_2} \overline{z_1' z_2'} \; . \tag{2.5g,h}$$

Since by definition,

$$\overline{z_1' z_2'} = \sigma_1^z \sigma_2^z C^{zz} \; , \tag{2.6a}$$

it is clear from (2.5a-h) that the wind-height and wind-wind covariances depend not only on derivatives of $C^{zz}$, but also on derivatives of either or both of $\sigma_1^z$ and $\sigma_2^z$ . The latter derivatives are assumed to be neglibible in conventional OI schemes. We retain these terms in the derivation to follow.

Taking the natural logarithm of (2.6a) gives

$$\log \overline{z_1' z_2'} = \log \sigma_1^z + \log \sigma_2^z + \log C^{zz} \; , \tag{2.6b}$$

and differentiating (2.6b) with respect to $\phi_1$ , say, gives

$$\frac{\partial}{\partial \phi_1} \overline{z_1' z_2'} = \overline{z_1' z_2'} \left( \frac{\partial \log C^{zz}}{\partial \phi_1} + \frac{\partial \log \sigma_1^z}{\partial \phi_1} \right) \tag{2.7a}$$

Differentiating (2.7a) with respect to $\lambda_2$ , say, gives

$$\frac{\partial^2}{\partial \phi_1 \partial \lambda_2} \overline{z_1' z_2'} = \overline{z_1' z_2'} \left[ \frac{\partial^2 \log C^{zz}}{\partial \phi_1 \partial \lambda_2} + \left( \frac{\partial \log C^{zz}}{\partial \phi_1} + \frac{\partial \log \sigma_1^z}{\partial \phi_1} \right) \left( \frac{\partial \log C^{zz}}{\partial \lambda_2} + \frac{\partial \log \sigma_2^z}{\partial \lambda_2} \right) \right] \tag{2.7b}$$

$$= \overline{z_1' z_2'} \left[ \frac{\partial^2 \log C^{zz}}{\partial \phi_1 \partial \lambda_2} + \left( \frac{\frac{\partial}{\partial \phi_1} \overline{z_1' z_2'}}{\overline{z_1' z_2'}} \right) \left( \frac{\frac{\partial}{\partial \lambda_2} \overline{z_1' z_2'}}{\overline{z_1' z_2'}} \right) \right] . \qquad (2.7c)$$

Substituting (2.7a,c) and similar expressions into (2.5a-h) then gives

$$\overline{u_1' z_2'} \Big/ \overline{z_1' z_2'} = \alpha_1 \left( \frac{\partial \log C^{zz}}{\partial \phi_1} + \frac{\partial \log \sigma_1^z}{\partial \phi_1} \right) , \qquad (2.8a)$$

$$\overline{z_1' u_2'} \Big/ \overline{z_1' z_2'} = \alpha_2 \left( \frac{\partial \log C^{zz}}{\partial \phi_2} + \frac{\partial \log \sigma_2^z}{\partial \phi_2} \right) , \qquad (2.8b)$$

$$\overline{v_1' z_2'} \Big/ \overline{z_1' z_2'} = \beta_1 \left( \frac{\partial \log C^{zz}}{\partial \lambda_1} + \frac{\partial \log \sigma_1^z}{\partial \lambda_1} \right) , \qquad (2.8c)$$

$$\overline{z_1' v_2'} \Big/ \overline{z_1' z_2'} = \beta_2 \left( \frac{\partial \log C^{zz}}{\partial \lambda_2} + \frac{\partial \log \sigma_2^z}{\partial \lambda_2} \right) , \qquad (2.8d)$$

$$\overline{u_1' v_2'} \Big/ \overline{z_1' z_2'} = \alpha_1 \beta_2 \frac{\partial^2 \log C^{zz}}{\partial \phi_1 \partial \lambda_2} + \left( \frac{\overline{u_1' z_2'}}{\overline{z_1' z_2'}} \right) \left( \frac{\overline{z_1' v_2'}}{\overline{z_1' z_2'}} \right) , \qquad (2.8e)$$

$$\overline{v_1' u_2'} \Big/ \overline{z_1' z_2'} = \beta_1 \alpha_2 \frac{\partial^2 \log C^{zz}}{\partial \lambda_1 \partial \phi_2} + \left( \frac{\overline{v_1' z_2'}}{\overline{z_1' z_2'}} \right) \left( \frac{\overline{z_1' u_2'}}{\overline{z_1' z_2'}} \right) , \qquad (2.8f)$$

$$\overline{u_1' u_2'} \Big/ \overline{z_1' z_2'} = \alpha_1 \alpha_2 \frac{\partial^2 \log C^{zz}}{\partial \phi_1 \partial \phi_2} + \left( \frac{\overline{u_1' z_2'}}{\overline{z_1' z_2'}} \right) \left( \frac{\overline{z_1' u_2'}}{\overline{z_1' z_2'}} \right) , \qquad (2.8g)$$

$$\overline{v_1' v_2'} \Big/ \overline{z_1' z_2'} = \beta_1 \beta_2 \frac{\partial^2 \log C^{zz}}{\partial \lambda_1 \partial \lambda_2} + \left( \frac{\overline{v_1' z_2'}}{\overline{z_1' z_2'}} \right) \left( \frac{\overline{z_1' v_2'}}{\overline{z_1' z_2'}} \right) , \qquad (2.8h)$$

Equations (2.8a-h) express the ratios of wind-height and wind-wind forecast error covariances to the height-height covariance, in terms of logarithmic derivatives of the correlation $C^{zz}$ and the standard deviations $\sigma_1^z$ and $\sigma_2^z$. For reasons of computational efficiency, the calculation of wind-height and wind-wind covariances (or wind-height and wind-wind correlations given below) should proceed as indicated: the ratios (2.8a-d) are calculated first, and then used in (2.8e-h), after which all the ratios may be multiplied by $\overline{z_1' z_2'}$ to give the wind-height and wind-wind covariances themselves.

The derivatives of $\log \sigma_1^z$ and $\log \sigma_2^z$, which are the terms neglected in conventional OI schemes, appear explicitly only in (2.8a-d). These terms may be evaluated numerically, and involve little computational overhead. For that matter, the derivatives of an analytically specified $\log C^{zz}$ may also be evaluated numerically, to any desired accuracy, by taking difference quotients on as fine a mesh as necessary. Such an approach is in general somewhat more expensive than using analytically derived expressions for the derivatives of $\log C^{zz}$ (see companion paper). The derivatives of $\log \sigma_1^z$ and $\log \sigma_2^z$ can only be evaluated on the mesh on which the analysis is performed, however, since $\sigma^z$ is known only on the analysis mesh.

Although the forecast error covariances (2.8a-h) are the basic quantities required by an OI scheme, for a variety of reasons the calculation is generally split into separate calculations of the forecast error standard deviations and correlations. The variances $(\sigma_1^u)^2$ and $(\sigma_1^v)^2$ are found by letting point $P_2$ approach point $P_1$ in (2.8g,h), which gives for the standard deviations $\sigma_1^u$ and $\sigma_1^v$,

$$\sigma_1^u = \sigma_1^z \left|\alpha_1\right| \lim_{P_2 \to P_1} \left[ \frac{\partial^2 \log C^{zz}}{\partial \phi_1 \partial \phi_2} + \left( \frac{\partial \log C^{zz}}{\partial \phi_1} + \frac{\partial \log \sigma_1^z}{\partial \phi_1} \right) \left( \frac{\partial \log C^{zz}}{\partial \phi_2} + \frac{\partial \log \sigma_2^z}{\partial \phi_2} \right) \right]^{1/2} \quad (2.9a)$$

$$\sigma_1^v = \sigma_1^z \left|\beta_1\right| \lim_{P_2 \to P_1} \left[ \frac{\partial^2 \log C^{zz}}{\partial \lambda_1 \partial \lambda_2} + \left( \frac{\partial \log C^{zz}}{\partial \lambda_1} + \frac{\partial \log \sigma_1^z}{\partial \lambda_1} \right) \left( \frac{\partial \log C^{zz}}{\partial \lambda_2} + \frac{\partial \log \sigma_2^z}{\partial \lambda_2} \right) \right]^{1/2} \qquad (2.9b)$$

Analogous formulas hold for $\sigma_2^u$ and $\sigma_2^v$ .

Equations (2.9a,b) can be simplified substantially. A general property of autocorrelation functions $C(P_1, P_2)$, where for the moment $P_1$ and $P_2$ are points in an arbitrary n-dimensional space, is that

$$\lim_{P_2 \to P_1} \frac{\partial C}{\partial \xi} = 0 \qquad (2.10a)$$

if C is in fact differentiable at $P_2 = P_1$, where $\xi$ is any coordinate of either $P_1$ or $P_2$. Since $\frac{\partial \log C}{\partial \xi} = \frac{1}{C} \frac{\partial C}{\partial \xi}$ and, by definition, $C = 1$ at $P_2 = P_1$, (2.10a) is equivalent to

$$\lim_{P_2 \to P_1} \frac{\partial \log C}{\partial \xi} = 0 \qquad . \qquad (2.10b)$$

In one dimension $(P_1, P_2) = (x_1, x_2)$, equation (2.10a) is just the statement that since, by definition, $|C| \leq 1$ and $C = 1$ when $x_2 = x_1$, it must be that $\frac{\partial C}{\partial x_2} \geq 0$ when $x_2 = x_1 - \varepsilon$ and $\frac{\partial C}{\partial x_2} \leq 0$ when $x_2 = x_1 + \varepsilon$, for all $\varepsilon > 0$ sufficiently small. Letting $\varepsilon \to 0$ implies

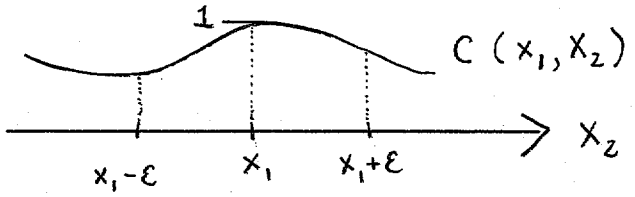


that $\frac{\partial C}{\partial x_2} = 0$ at $x_2 = x_1$ if C is differentiable there. By definition, $C(x_1, x_2) = C(x_2, x_1)$, so $\frac{\partial C}{\partial x_1} = 0$ at $x_2 = x_1$ also.

In OI we need only consider differentiable height-height correlation functions $C^{zz}$, since we must always take derivatives of $C^{zz}$. According to (2.10b), equations (2.9a,b) are therefore equivalent to

$$\sigma_1^u = \sigma_1^z \, |\alpha_1| \left[ \lim_{P_2 \to P_1} \frac{\partial^2 \log C^{zz}}{\partial \phi_1 \, \partial \phi_2} + \left( \frac{\partial \log \sigma_1^z}{\partial \phi_1} \right)^2 \right]^{1/2} , \qquad (2.11a)$$

$$\sigma_1^v = \sigma_1^z \, |\beta_1| \left[ \lim_{P_2 \to P_1} \frac{\partial^2 \log C^{zz}}{\partial \lambda_1 \, \partial \lambda_2} + \left( \frac{\partial \log \sigma_1^z}{\partial \lambda_1} \right)^2 \right]^{1/2} , \qquad (2.11b)$$

and similarly for $\sigma_2^u$ and $\sigma_2^v$. Therefore, retaining the terms involving horizontal derivatives of $\sigma^z$ always increases $\sigma^u$ and $\sigma^v$. This means that in regions of strong gradients of $\sigma^z$, the wind field forecast will be relied on less heavily, and nearby observations will be weighted more heavily. Notice also in (2.11a,b) that the standard deviations $\sigma_1^u$ and $\sigma_1^v$ depend on the curvatures of log $C^{zz}$ in the coordinate directions at $P_2 = P_1$, but are otherwise independent of $C^{zz}$.

Finally, we obtain the relationships among forecast error correlations. Defining

$$\gamma_i \equiv \frac{\sigma_i^z \, \alpha_i}{\sigma_i^u} , \quad \delta_i \equiv \frac{\sigma_i^z \, \beta_i}{\sigma_i^v} , \qquad (2.12a,b)$$

we have from (2.11a,b) that

$$\gamma_1 = (\text{sign } \alpha_1) \left[ \lim_{P_2 \to P_1} \frac{\partial^2 \log C^{zz}}{\partial \phi_1 \, \partial \phi_2} + \left( \frac{\partial \log \sigma_1^z}{\partial \phi_1} \right)^2 \right]^{-1/2} , \qquad (2.13a)$$

$$\delta_1 = (\text{sign } \beta_1) \left[ \lim_{P_2 \to P_1} \frac{\partial^2 \log C^{zz}}{\partial \lambda_1 \, \partial \lambda_2} + \left( \frac{\partial \log \sigma_1^z}{\partial \lambda_1} \right)^2 \right]^{-1/2} , \qquad (2.13b)$$

and similarly for $\gamma_2$ and $\delta_2$, where

$$\text{sign } x \equiv \frac{x}{|x|} . \qquad (2.14)$$

From (2.8a-h) and (2.12a,b) we then have

$$C^{uz}/C^{zz} = \gamma_1 \left( \frac{\partial \log C^{zz}}{\partial \phi_1} + \frac{\partial \log \sigma_1^z}{\partial \phi_1} \right) , \qquad (2.15a)$$

$$C^{zu}/C^{zz} = \gamma_2 \left( \frac{\partial \log C^{zz}}{\partial \phi_2} + \frac{\partial \log \sigma_2^z}{\partial \phi_2} \right) , \qquad (2.15b)$$

$$C^{vz}/C^{zz} = \delta_1 \left( \frac{\partial \log C^{zz}}{\partial \lambda_1} + \frac{\partial \log \sigma_1^z}{\partial \lambda_1} \right) , \qquad (2.15c)$$

$$C^{zv}/C^{zz} = \delta_2 \left( \frac{\partial \log C^{zz}}{\partial \lambda_2} + \frac{\partial \log \sigma_2^z}{\partial \lambda_2} \right) , \qquad (2.15d)$$

$$C^{uv}/C^{zz} = \gamma_1 \delta_2 \frac{\partial^2 \log C^{zz}}{\partial \phi_1 \partial \lambda_2} + \frac{C^{uz}}{C^{zz}} \frac{C^{zv}}{C^{zz}} , \qquad (2.15e)$$

$$C^{vu}/C^{zz} = \delta_1 \gamma_2 \frac{\partial^2 \log C^{zz}}{\partial \lambda_1 \partial \phi_2} + \frac{C^{vz}}{C^{zz}} \frac{C^{zu}}{C^{zz}} , \qquad (2.15f)$$

$$C^{uu}/C^{zz} = \gamma_1 \gamma_2 \frac{\partial^2 \log C^{zz}}{\partial \phi_1 \partial \phi_2} + \frac{C^{uz}}{C^{zz}} \frac{C^{zu}}{C^{zz}} , \qquad (2.15g)$$

$$C^{vv}/C^{zz} = \delta_1 \delta_2 \frac{\partial^2 \log C^{zz}}{\partial \lambda_1 \partial \lambda_2} + \frac{C^{vz}}{C^{zz}} \frac{C^{zv}}{C^{zz}} . \qquad (2.15h)$$

Equations (2.15a-h) are quite similar in form to the covariance formulas (2.8a-h). Notice, however, that the correlations (2.15a-h) depend on the signs of $\alpha_i$ and $\beta_i$, through (2.13a,b), but not on the values of $\alpha_i$ and $\beta_i$. In

particular, the correlations are independent of the geostrophy coefficient $G_i$ wherever $G_i \neq 0$.

## III. Discussion of OI Statistical Relationships

Several remarks are pertinent at this point. First, recall that all the statistical relationships above have been formulated in terms of logarithmic derivatives, primarily for mathematical convenience. In fact, $C^{zz}$ is taken to be the exponential of a rather simple function in most OI schemes ($C^{zz}$ is Gaussian at NMC), so that the appearance of log $C^{zz}$ in the statisitical relationships is quite natural. Furthermore, the NMC OI system stores $\sigma^z$ in the form of spectral coefficients of log $\sigma^z$, so that computer calculation of derivatives of log $\sigma^z$ is particularly simple.

It is a standard assumption in OI formulations that $C^{zz}$ separates into horizontal and vertical parts:

$$C^{zz}(\lambda_1, \phi_1, p_1; \lambda_2, \phi_2, p_2) = H^{zz}(\lambda_1, \phi_1; \lambda_2, \phi_2) V(p_1; p_2) \quad (3.1)$$

It follows immediately that horizontal derivatives of log $C^{zz}$ are identical to horizontal derivatives of log $H^{zz}$, i.e.,

$$\frac{\partial}{\partial \phi_i} \log C^{zz} = \frac{\partial}{\partial \phi_i} \log H^{zz} , \quad (3.2a)$$

$$\frac{\partial}{\partial \lambda_i} \log C^{zz} = \frac{\partial}{\partial \lambda_i} \log H^{zz} , \quad (3.2b)$$

and likewise for the second derivatives. This simplifies the main results obtained so far: in each of equations (2.8a-h), (2.11a,b), (2.13a,b), and (2.15a-h), log $C^{zz}$ may be replaced by log $H^{zz}$.

Notice, however, that (3.1) does not imply that

$$C^{qr}(\lambda_1, \phi_1, p_1; \lambda_2, \phi_2, p_2) = H^{qr}(\lambda_1, \phi_1; \lambda_2, \phi_2)\, V(p_1; p_2) \quad (3.3)$$

for the remaining correlations, as it does in conventional OI. If the terms involving derivatives of log $\sigma^z$ were neglected in (2.15a-h), then clearly the right-hand-sides of those equations would be independent of the vertical coordinate. Thus, the left-hand-sides of (2.15 a-h) would be independent of the vertical coordinate also, from which (3.3) would follow, and the left-hand-sides could be replaced by ratios $H^{qr}/H^{zz}$. When the terms involving log $\sigma^z$ are retained in (2.15a-h), however, the right-hand-sides do depend on the vertical coordinate, since $\sigma^z$ is in general not separable into horizontal and vertical parts. Thus, the only computational simplification to which (3.1) leads when derivatives of log $\sigma^z$ are retained in OI is the replacement (3.2) of derivatives of log $C^{zz}$ by those of log $H^{zz}$. This simply means that derivatives of log $\sigma^z$, and therefore, relationships (2.8a-h), (2.11a,b), (2.13 a,b,), and (2.15 a-h), must be evaluated on individual pressure surfaces.

A few remarks concerning the geostrophic assumption itself are in order. It is by now a well-known fact that any linear relationship satisfied by forecast errors is satisfied automatically by the analysis increments also, provided no contradictory assumptions are made in deducing the forecast error covariances from the forecast errors themselves. (For various precise versions of this statement, see Petersen, 1973; Cohn, 1982, pp. 84-87, 129-131; and Phillips, 1982.) Thus, if our covariance formulas (2.8a-h), or equivalently the variance formulas (2.11a,b) and correlation formulas (2.15a-h), are used as the basis of an OI scheme, then regardless of the assumed form of $C^{zz}$, the analysis increments will satisfy the geostrophic relationships (2.1, 2.2). That is,

the analysis increments will be geostrophic where G = 1 and "subgeostrophic" where G < 1.

We show in the following sections that inclusion of derivatives of log $\sigma^2$ in the OI statistical relationships has a large effect upon the derived statistics. Thus, neglect of these terms would contradict substantially the original assumption (2.1, 2.2) of geostrophic forecast errors. Conventional OI schemes, in which these terms are neglected, therefore do not have geostrophic (or "subgeostrophic") analysis increments, at least in regions where $\sigma^2$ is changing rapidly. Part of our motivation in this work is, in fact, to develop a more self-consistent OI scheme, which in light of the geostrophic assumption means a scheme which yields geostrophic analysis increments. While the merit of the geostrophic assumption itself is questionable (e.g., see the following paragraphs), analysis increments with predictable behavior are certainly preferable to increments which behave unpredictably.

One additional assumption contradicting (2.1, 2.2) is made at NMC. This assumption is motivated by the following argument. Notice in (2.2) that if $G \to 0$ as $\phi \to 0$ faster than $f = 2\Omega \sin\phi \to 0$, then $\alpha = \beta = 0$ at $\phi = 0$. In fact, at NMC, $\alpha$ and $\beta$ are taken to be zero equatorward of 10°. But then, if we follow assumption (2.1), the forecast errors in the wind field are zero in that region. Consequently, the forecast error covariances (2.8a-h) and standard deviations (2.11a,b) are zero in that region. (Also, the correlations (2.15a-h) are undefined when $\alpha = \beta = 0$ due to the appearance of the factors $\gamma$ and $\delta$ which, according to (2.13a,b) and (2.14) are not defined when $\alpha = \beta = 0$. We may take the correlations to be zero in this case, i.e., we may define sign $X = 0$ when $X = 0$, because in OI the correlations are eventually multiplied by (zero) standard deviations to give (zero) covariances.)

This simply means that the forecast is perfect in this region, and OI would use no observations to update the forecast there.

This is clearly an undesirable situation. The remedy used at NMC is that, as $G \rightarrow 0$, the standard deviations $\sigma^u$ and $\sigma^v$ are augmented by an amount which tends to a nonzero constant at the equator. The covariances are calculated by multiplying these augmented standard deviations by the usual geostrophic correlations. The result, of course, is that analysis increments do not satisfy (2.1, 2.2) in the tropics, and it is difficult to say what kind of relationships they do satisfy. This fact, in conjunction with the neglect of derivatives of $\sigma^z$ in the OI formulation, is likely to cause poor tropical analyses.

A more natural way to remedy this situation would be simply to modify the geostrophic assumption which, after all, is the cause of the dilemma. Daley (1983), for example, has suggested the introducton of some divergence into the basic assumption. Equations (2.1, 2.2), as they stand, imply that there is no error in the forecast of the divergent wind, which is not a good assumption in the tropics.

As a final remark, we note that is it less expensive to calculate only covariances (2.8a-h), which are the statistics actually required by OI, rather than to calculate separately the standard deviations (2.11a,b) and correlations (2.15a-h). This is currently not done at NMC, at least in part because of the aforementioned process of augmenting $\sigma^u$ and $\sigma^v$ in the tropics.

## IV. The Magnitude of $\sigma^z$- Gradient Effects

To develop insight into the effect of including horizontal gradients of $\sigma^z$ in an OI formulation, we now calculate some of the OI statistical relationships in case $C^{zz}$ is a Gaussian function of spherical distance. Both in this section

and the next, we use the variance formulas (2.11) and correlation formulas (2.15) and we contrast the values they yield in the absence and in the presence of gradients of $\sigma^z$. For the variances, the comparison is not strictly one between the current NMC scheme and a scheme which accounts for variability of $\sigma^z$, since the current NMC practice also involves augmenting the variances in the tropics, as discussed in the previous section. The comparison for correlations, however, can be regarded as such a strict comparison, since the current NMC scheme does not alter the correlations in the tropics.

We take

$$C^{zz} = H^{zz}(\lambda_1, \phi_1 ; \lambda_2 \phi_2)\, V(p_1; p_2) \tag{4.1}$$

as in (3.1), and we specify a Gaussian horizontal correlation

$$H^{zz} = e^{-\frac{1}{2} b s^2} \tag{4.2}$$

where s is the angle subtended at the center of the earth by points $P_1$ and $P_2$,

$$s = \arccos [\sin \phi_1 \sin \phi_2 + \cos \phi_1 \cos \phi_2 \cos (\lambda_1 - \lambda_2)], \tag{4.3}$$

and

$$b = 2a^2 / d_o^2 \tag{4.4}$$

Here a is the radius of the earth, so that as is the spherical distance between points $P_1$ and $P_2$, and $d_o$ is the correlation distance (currently $d_o = \frac{1}{\sqrt{2}} \times 10^3$ km at NMC). We examine first the effect of horizontal gradients of $\sigma^z$ upon $\sigma^u$. One can show for $C^{zz}$ given by (4.1-4.4) that

$$\lim_{P_2 \to P_1} \frac{\partial^2 \log C^{zz}}{\partial \phi_1 \, \partial \phi_2} = b . \qquad (4.5)$$

In fact, equation (4.5) still holds if (4.3) is replaced by various approximations to the spherical distance, including the one in current use at NMC (see companion paper). From (2.11a) and (4.5) we have

$$\sigma_1^u = \sigma_1^z \, |\alpha_1| \left[ b + \left( \frac{\partial \log \sigma_1^z}{\partial \phi_1} \right)^2 \right]^{1/2} . \qquad (4.6)$$

When gradients of $\sigma^z$ are neglected (or are small), it follows that $|\alpha| \, b^{1/2} = \frac{|\alpha| \sqrt{2} a}{d_o}$ is the constant of proportionality between $\sigma^u$ and $\sigma^z$. Therefore, decreasing the correlation distance $d_o$ always increases $\sigma^u$ (and $\sigma^v$). Furthermore, retaining gradients of $\sigma^z$ always increases $\sigma^u$ (and $\sigma^v$). This was already noted in Section II.

To ascertain the magnitude of the latter effect, let

$$R_1^u \equiv \frac{\sigma_1^u \text{ with gradient term}}{\sigma_1^u \text{ without gradient term}} \qquad (4.7a)$$

$$= \left[ 1 + \frac{1}{b} \left( \frac{\partial \log \sigma_1^z}{\partial \phi_1} \right)^2 \right]^{1/2} . \qquad (4.7b)$$

Further, from (4.4) we have that

$$R_1^u = \left[ 1 + \frac{1}{2} \left( \frac{d_o}{\sigma_1^z} \frac{\partial \sigma_1^z}{a \partial \phi_1} \right)^2 \right]^{1/2} \qquad (4.7c)$$

$$= \left[ 1 + \frac{1}{2} \left( \frac{\Delta \sigma_1^z}{\sigma_1^z} \right)^2 \right]^{1/2} , \qquad (4.7d)$$

where $\Delta \sigma_1^z$ denotes the instantaneous change in $\sigma_1^z$ per meridional distance $d_o$. Referring to Fig. 1, we see that contours are frequently as close together

as 100 km, in which case $\Delta\sigma_1^z$ = 35 m, since the contour interval is 5 m and $d_0 \cong$ 700 km. This occurs, for example, at the 30 m contour near 25°N, 330°W. Here we have $\frac{\Delta\sigma_1^z}{\sigma_1^z} = \frac{35}{30}$, so that

$$R_1^v = 1.30 \quad . \tag{4.8}$$

Retention of gradients of $\sigma^z$ in OI can increase the magnitude of $\sigma^v$ and $\sigma^v$ by up to about 30%.

Next we examine the effect of gradients of $\sigma^z$ upon the correlation function $C^{uz}$. Consider points $P_1$ and $P_2$ for which $C^{uz}(P_1,P_2) = 0$ when gradients of $\sigma_1^z$ are neglected. Then when these gradients are included we have from (2.15a, 2.13a, 4.5) that

$$C^{vz}/C^{zz} = (\text{sign}\,\alpha_1)\left[b+\left(\frac{\partial \log\sigma_1^z}{\partial\phi_1}\right)^2\right]^{-1/2}\frac{\partial \log\sigma_1^z}{\partial\phi_1} \tag{4.9a}$$

or, with (4.7b),

$$C^{vz} = (\text{sign}\,\alpha_1)\left(\text{sign}\,\frac{\partial\sigma_1^z}{\partial\phi_1}\right)\sqrt{1-\frac{1}{(R_1^v)^2}}\;C^{zz} \tag{4.9b}$$

That is, upon including the effect of variability of $\sigma_1^z$, the zero-line of $C^{uz}$ instead has values proportional to $C^{zz}$. The constant of proportionality can be quite large: when $R^u_1$ = 1.3, for example, we have

$$C^{vz} = 0.64\,(\text{sign}\,\alpha_1)\left(\text{sign}\,\frac{\partial\sigma_1^z}{\partial\phi_1}\right)C^{zz} \quad . \tag{4.9c}$$

Thus, at the origin $P_2 = P_1$, which does lie on the zero-line of the conventional $C^{uz}$ (Fig. 3a), we now have $C^{uz} = \pm\, 0.64$. This is a very large effect, which should have significant impact on OI analyses.

The nature of this effect is actually independent of the height-height correlation function $C^{zz}$. Where the logarithmic first derivatives of $\sigma^z$ are

large compared to those of $C^{zz}$, and where the squares of the logarithmic first derivatives of $\sigma^z$ are large compared to the curvatures of log $C^{zz}$ at the origin $P_2 = P_1$, it follows immediately from (2.13, 2.15) that

$$C^{uz} \cong (\text{sign}\,\alpha_1)\left(\text{sign}\,\frac{\partial \sigma_1^z}{\partial \phi_1}\right) C^{zz} \tag{4.10a}$$

$$C^{zu} \cong (\text{sign}\,\alpha_2)\left(\text{sign}\,\frac{\partial \sigma_2^z}{\partial \phi_2}\right) C^{zz} \tag{4.10b}$$

$$C^{vz} \cong (\text{sign}\,\beta_1)\left(\text{sign}\,\frac{\partial \sigma_1^z}{\partial \lambda_1}\right) C^{zz} \tag{4.10c}$$

$$C^{zv} \cong (\text{sign}\,\beta_2)\left(\text{sign}\,\frac{\partial \sigma_2^z}{\partial \lambda_2}\right) C^{zz} \tag{4.10d}$$

$$C^{uv} \cong (\text{sign}\,\alpha_1)(\text{sign}\,\beta_2)\left(\text{sign}\,\frac{\partial \sigma_1^z}{\partial \phi_1}\right)\left(\text{sign}\,\frac{\partial \sigma_2^z}{\partial \lambda_2}\right) C^{zz} \tag{4.10e}$$

$$C^{vu} \cong (\text{sign}\,\beta_1)(\text{sign}\,\alpha_2)\left(\text{sign}\,\frac{\partial \sigma_1^z}{\partial \lambda_1}\right)\left(\text{sign}\,\frac{\partial \sigma_2^z}{\partial \phi_2}\right) C^{zz} \tag{4.10f}$$

$$C^{uu} \cong (\text{sign}\,\alpha_1)(\text{sign}\,\alpha_2)\left(\text{sign}\,\frac{\partial \sigma_1^z}{\partial \phi_1}\right)\left(\text{sign}\,\frac{\partial \sigma_2^z}{\partial \phi_2}\right) C^{zz} \tag{4.10g}$$

$$C^{vv} \cong (\text{sign}\,\beta_1)(\text{sign}\,\beta_2)\left(\text{sign}\,\frac{\partial \sigma_1^z}{\partial \lambda_1}\right)\left(\text{sign}\,\frac{\partial \sigma_2^z}{\partial \lambda_2}\right) C^{zz} \tag{4.10h}$$

The example we have given indicates that realistic $\sigma^z$ fields are in some regions rather close to this asymptotic situation. We attempt to quantify this statement further in the next section.

## V. Correlation Functions for Simulated $\sigma^z$ Fields

At NMC, the height-field forecast error standard deviation $\sigma^z$ is obtained by adding to the estimated analysis error variance a quantity representing the growth of error variance over the six-hour forecast period. The estimated analysis error variance is a by-product of the OI analysis procedure. It is computed at each analysis point and is a function of the amount, quality and distribution of the data near each analysis point.

Figure 1 is a map of the estimated forecast error standard deviation of height at 500 mb for 00Z on September 10, 1984. We see that there are a number of areas where $\sigma^z$ changes quite rapidly. For instance, there is a bulls-eye feature centered over the Amazon region. The contours surrounding this region represent the change in $\sigma^z$ from the data-sparse Amazon basin to the areas surrounding it where there are more plentiful data. There is also a similar area of less circular contours surrounding the region of the Sahara Desert. Less densely packed are the contours visible off the western coast of North America, which indicate the transition zone between the dense, high quality radiosonde data prevalent over the continent, and the oceanic region dominated by satellite data which are assumed to be of lesser quality.

We shall use idealized representations of these three regions to investigate the impact of accounting for gradients of the height-field forecast error standard deviations. Our sample forecast error standard deviation fields will be constructed using the simple delta-like function

$$g(x) = \frac{\alpha}{1 + \alpha^2 \left(\frac{x - x_0}{\beta}\right)^{2p}} \qquad (5.1)$$

In this equation, $\alpha$ controls the amplitude, $\beta$ is a scale factor, $X_o$ locates the center of the peak, and p broadens the peak. To represent a two-dimensional forecast error standard deviation field, g( $\phi$ ) and g( $\lambda$ ) are multiplied together. A separate set of parameters is specified for each direction. Also, since nowhere on the globe does the forecast error standard deviation approach zero, a constant $C_0$ is added to the product. The equation used to specify the height forecast error standard deviation field is

$$\sigma^z(\lambda,\phi) = \frac{\alpha_\lambda}{1+\alpha_\lambda^2\left(\frac{\lambda-\lambda_o}{\beta_\lambda}\right)^{2p_\lambda}} \cdot \frac{\alpha_\phi}{1+\alpha_\phi^2\left(\frac{\phi-\phi_o}{\beta_\phi}\right)^{2p_\phi}} + C_o \qquad (5.2)$$

Figure 2 presents three sample forecast error standard deviation fields. To facilitate comparisons and to minimize spherical distortion, each field is centered at 30°N latitude. In each case, we will calculate correlations between a centrally-located analysis point and points throughout the region. Figure 2a represents the feature shown in Figure 1 centered over northern South America. The parameters used in equation (5.2) to produce this pattern are listed below.

| | | | | |
|---|---|---|---|---|
| $\alpha_\phi = 7.5$ | $\beta_\phi = 15.0$ | $\phi_o = 30.0$ | $p_\phi = 4.0$ | $C_o = 29.0$ |
| $\alpha_\lambda = 7.5$ | $\beta_\lambda = 15.0$ | $\lambda_o = 100.0$ | $p_\lambda = 4.0$ | |

Figure 2b represents the portion of the $\sigma^z$ field between the Mediterranean and the Sahara in Figure 1. The parameters specifying this field are

| | | | | |
|---|---|---|---|---|
| $\alpha_\phi = 8.5$ | $\beta_\phi = 40.0$ | $\phi_o = 10.0$ | $p_\phi = 3.0$ | $C_o = 19.0$ |
| $\alpha_\lambda = 8.5$ | $\beta_\lambda = 90.0$ | $\lambda_o = 100.0$ | $p_\lambda = 3.0$ | |

Figure 2c is an idealized representation of the broader gradient of $\sigma^z$ located off the coast of the southwestern United States. The parameters for this field are

$\alpha_\phi = 5.0$ $\beta_\phi = 70.0$ $\phi_o = -15.0$ $p_\phi = 4.0$ $C_o = 10.0$

$\alpha_\lambda = 5.0$ $\beta_\lambda = 90.0$ $\lambda_o = 100.0$ $p_\lambda = 4.0$

In Figures 3a-d we show the uz, uv, uu and vv correlations (2.15a,e,g,h) centered at 30°N latitude for the case in which gradients of $\sigma^z$ are neglected, using the correlation function given by equations (4.1-4.4). Results using other formulas in place of (4.3) are described in the companion paper. The figures described below, in which gradients of $\sigma^z$ are retained, will be compared to Figs. 3a-d. In all the figures, point $P_1$ is the analysis point, located in the center of the frame, and point $P_2$ is the variable point.

Figures 4a-d display the same forecast error correlation functions shown in Figs. 3a-d, except that they include the effect of the height forecast error standard deviation field shown in Figure 2a. Figures 4a and 3a, representing the uz forecast error correlation, appear to be identical. To explain this, notice that the only derivative of $\sigma^z$ in equation (2.15a) is the derivative of log $\sigma^z$ with respect to latitude at location 1, the analysis point. Figure 2a shows that this derivative is zero.

Before discussing the appearance of Figure 4b, the uv correlation function corresponding to Figure 2a, we examine equation (2.15e) to predict where changes should be most noticable. The two terms involving derivatives of $\sigma^z$ are with respect to latitude at point 1, the analysis point, and with respect to longitude at point 2. We have already seen that the former derivative is zero. The latter is largest in the area bordered by 40 and 20 degrees latitude on the north and south and 115 and 105 degrees longitude on the west and east, and also in a box with the same northern and southern extents and with east and west borders of 85 and 95 degrees west longitude. Comparison of Figures 4b and 3b reveals significant differences in these two areas.

The equation for the uu correlation (2.15g) contains derivatives of with respect to latitude only. The areas in which $\sigma^z$ varies most with latitude in Figure 2a coincide with the location of the negative lobes of the uu correlation in Figure 3c. In Figure 4c, these lobes have increased in amplitude.

Equation (2.15h), used to construct the vv correlations in Figure 4d, only has derivative terms with respect to longitude. Therefore, we should see the greatest changes in the areas of the largest east-west gradient in Figure 2a. Figure 4d shows the two side lobes of the vv correlation, which are located in the regions of the sharpest longitudinal gradients of $\sigma^z$, to be of significantly higher amplitude than the corresponding vv correlation in Figure 3d.

Figure 2b represents a case in which the analysis point is located in the midst of a north-south gradient of $\sigma^z$ similar to the gradient seen in Figure 1 between the Mediterranean and the Sahara. With a field such as this, all the derivatives of $\sigma^z$ with respect to longitude will be zero and the only terms to contribute will be those involving a change of $\sigma^z$ with latitude.

Figure 5a, compared to Figure 3a, shows the radical transformation of the uz correlation that occurred from assuming the field of $\sigma^z$ in Figure 2b. The zero line has been shifted about 2 degrees northward. The southern positive lobe has increased in amplitude and area while the northern negative lobe has lost intensity and spatial extent. One effect is that the correlation of u and z forecast errors at the analysis point, which is zero using the correlation equations in operational use today (see Figure 3a), would now be 0.4. This is a substantial change.

The forecast error standard deviation field in Figure 2b produces much the same effect with the uv correlation function. In Figure 5b, the two lobes south

of the zero line have increased in amplitude, the two lobes north of the zero line have lost intensity and the zero line itself has been moved northward by about 2 degrees. This change affects greatly the weight that an observation would be assigned.

The terms accounting for non-homogeneous height forecast error standard deviations in the uu correlation equations are derivatives with respect to latitude only. Therefore, we should see some difference between the uu correlations in Figure 5c and those in Figure 3c. There are small differences everywhere but the areas where they are most noticable are the two negative lobes. The northern negative lobe has reduced in amplitude and the southern negative lobe has increased in amplitude.

The vv correlation in Figure 5d is identical to the one displayed in Figure 3d because the vv correlation equation (2.15h) contains derivatives of $\sigma^z$ with respect to longitude only. The $\nabla^z$ field in Figure 2b is independent of longitude.

Figure 2c, the last of the height forecast error standard deviation fields that we shall examine here, is similar to the previous one (Figure 2b), except that it represents a much smaller gradient. It is meant to represent the gradient present in Figure 1 off the southwest coast of the United States and Mexico. Again, the analysis point is in the center of the figure at 30°N. Figures 6a-d present the correlations calculated using the $\sigma^z$ field in Figure 2c. Here we expect an effect similar to that shown in Figures 5a-d, but with smaller magnitude.

Figure 6a does show an effect similar to that observed in Figure 5a. The zero line is moved northward but only by about one degree in this case.

Also, the reduction of amplitude in the northern lobe and the increase of amplitude in the southern lobe is less. The same effect is seen in Figure 6b, with the uv correlation function. There is a change in the uu correlation shown in Figure 6c that is similar to the change seen in Figure 5c, but with smaller magnitude. The vv correlation in Figure 6d is the same as that in Figures 3d and 5d.

## VI. Summary and Conclusions

The dominant feature on maps of the height-field forecast error standard deviation, $\sigma^z$, is the presence of strong horizontal gradients of $\sigma^z$ near boundaries separating data-dense and data-sparse regions. This fact is neglected in the forecast error covariance formulas which are fundamental to the OI analysis system at NMC. We have derived new formulas for the forecast error covariances which fully account for the spatial variability of $\sigma^z$. Apart from the presence of a few easily-calculated additional terms, these formulas are identical to those used currently in the OI system.

A simple analysis of the new formulas demonstrates that the effect of variability of $\sigma^z$ is large in many regions. The effect always increases the wind-field forecast error standard deviations. The wind-height and wind-wind forecast error correlations lose the homogeneity and isotropy properties they possess in the operational OI system. In fact, these correlations all asymptote to the height-height forecast error correlation with increasing gradients of $\sigma^z$. Plots based on simulated $\sigma^z$ fields demonstrate that gradients of $\sigma^z$ encountered in several regions of the globe place the wind-height and wind-wind correlations well within this asymptotic regime.

Our sole assumption in this work is identical to the assumption upon which the current operational OI system is based: forecast errors are geostrophic in extratropical regions, and "subgeostrophic" in the tropics. We have pointed out that if the spatial variability of $\sigma^2$ is accounted for in the OI formulation, then the actual analysis increments will also be geostrophic in extratropical regions. We have also shown that the basic assumption leads to inconsistencies in the covariance relationships for tropical regions. A modification of the basic assumption which accounts for forecast error in the divergent wind should both remove these inconsistencies and enhance the likely benefit of accounting for the spatial variability of $\sigma^2$.

Acknowledgements. This work was motivated, in part, by comments of A. Lorenc at one of the joint NMC/GLAS/UM Seminars on Data Assimilation. We wish to thank M. Ghil for his advice and for his role in initiating this work, R. McPherson for his generous guidance, and D. Parrish for his helpful comments. We also thank M. Chapman for typing this manuscript.

## REFERENCES

Bergman, K., 1979: Multivariate analysis of temperatures and winds using optimum interpolation. Mon. Wea. Rev., 107, 1432-1444.

Cohn, S. E., 1982: Methods of sequential estimation for determining initial data in numrical weather prediction. Ph.D. thesis, Courant Insitutute of Mathematical Sciences Report No. CI-6-82, New York University, 183 pp.

Daley, R., 1983: Spectral characteristics of the ECMWF objective analysis system. Technical Report No. 40, European Center for Medium Range Weather Forecasts, Reading, England, 119 pp.

Lorenc, A., 1981: A global three-dimensional multivariate statistical interpolation scheme. Mon. Wea. Rev., 109, 701-721.

McPherson, R. D., K. H. Bergman, R. E. Kistler, G. E. Rasch and D. S. Gordon, 1979: The NMC operational global data assimilation system. Mon. Wea. Rev., 107, 1445-1461.

Morone, L. L. and S. E. Cohn, 1984: The effect of spherical distance approximations upon OI forecast error correlations. Office Note 297, National Meteorological Center, Washington, D.C., 20233.

Peterson, D. P., 1973: Transient suppresion in optimal sequential analysis. J. Appl. Meteor., 12, 437-440.

Phillips, N. A., 1982: On the completeness of multivariate optimum interpolation for large-scale meteorological analysis. Mon. Wea. Rev., 110, 1329-1334.

Rutherford, I. D., 1976: An operational three-dimensional multivariate statistical objective analysis scheme. Proceedings of the JOC Study Group Conference on Four-Dimensional Data Assimilation, Paris, November 17-21, 1975. The GARP Programme on Numerical Experimentation, Report No. 11, January 1976.

Schlatter, T. W., 1975: Some experiments with a multivariate statistical objective analysis scheme. Mon. Wea. Rev., 103, 246-257.

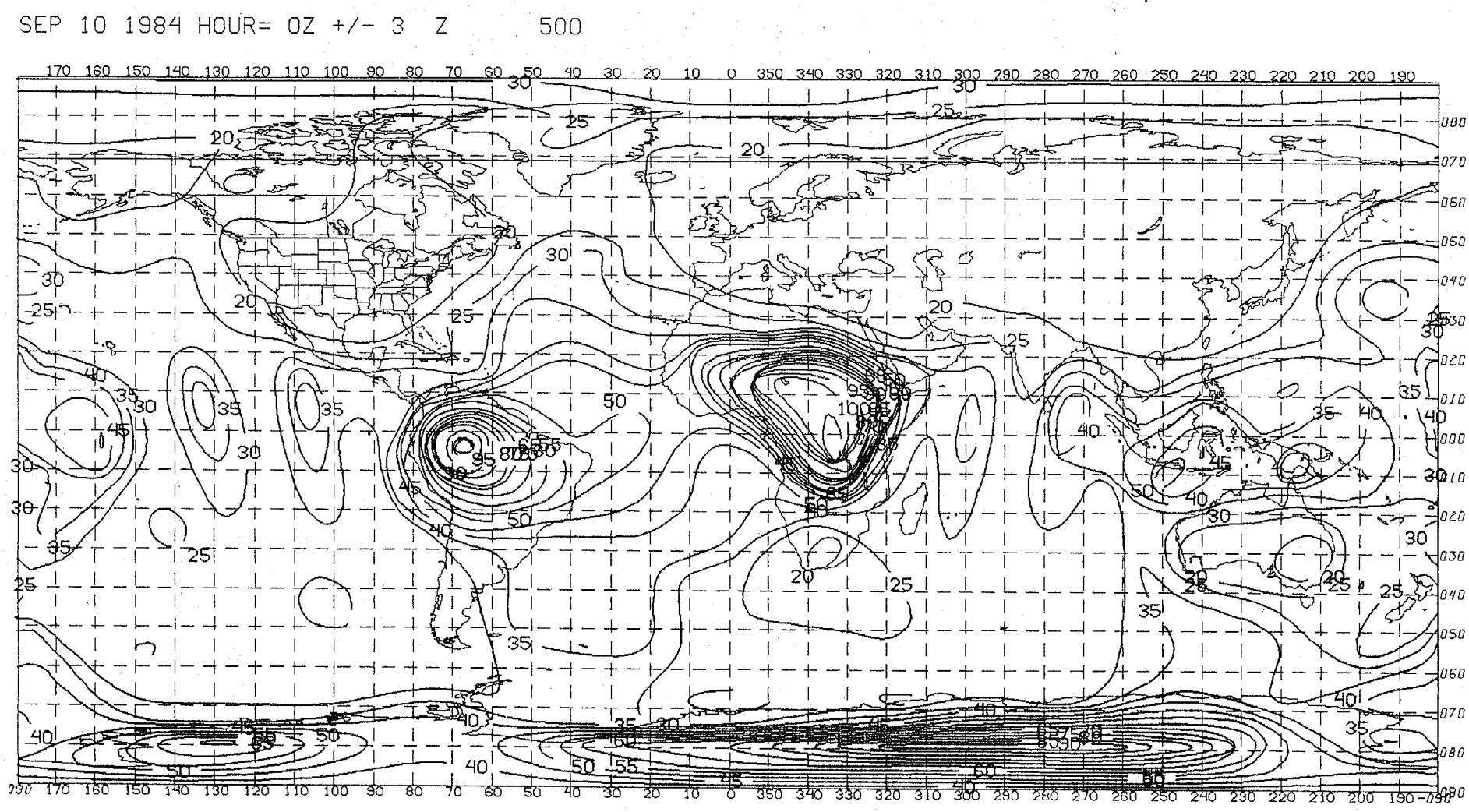


Figure 1. 500 mb height forecast error standard deviation for 00Z September 10, 1984 as derived from NMC's optimum interpolation analysis procedure. Contour interval is 5 meters.

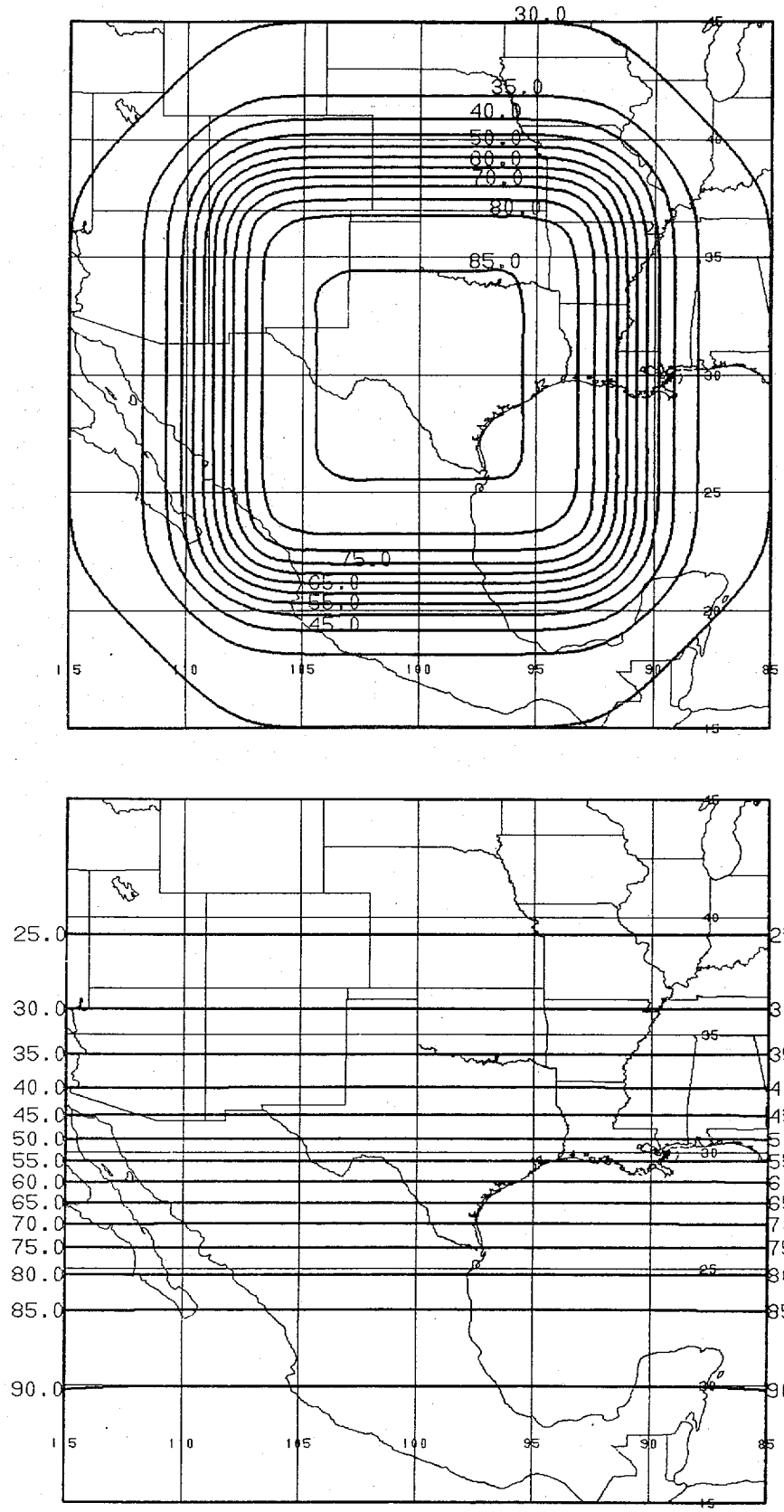


Figure 2. Sample height forecast error standard deviation fields representing three features seen in Figure 1: (a) the bullseye centered over northern South America, (b) the steep gradient between the Mediterranean Sea and the Sahara Desert and (c) the broader gradient off the southwestern coast of the United States.

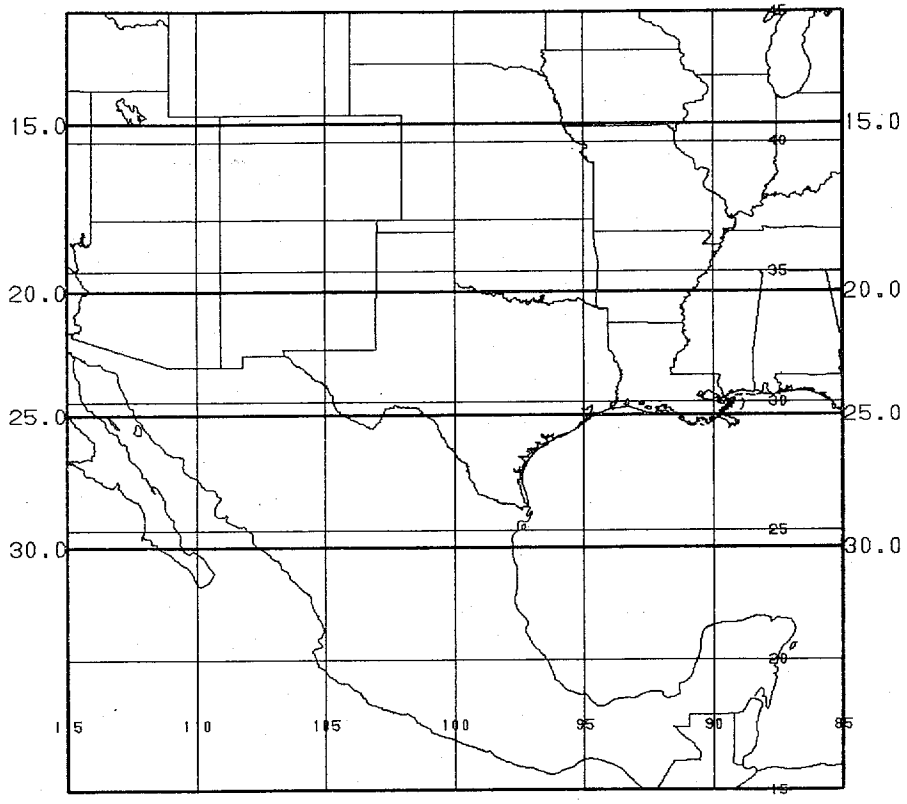


(c)

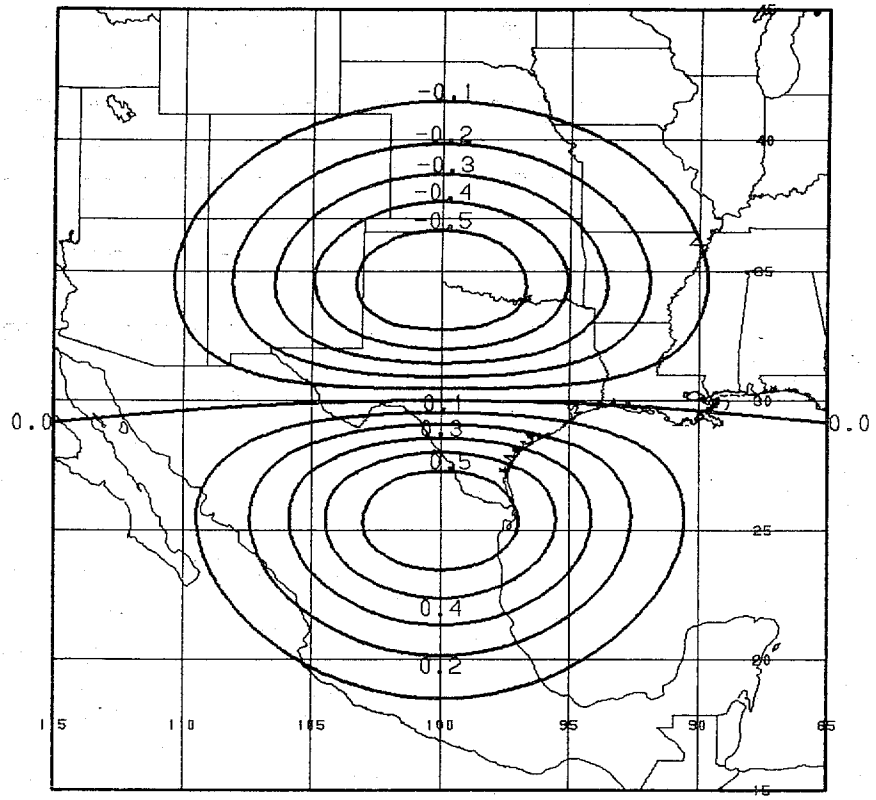


(a)

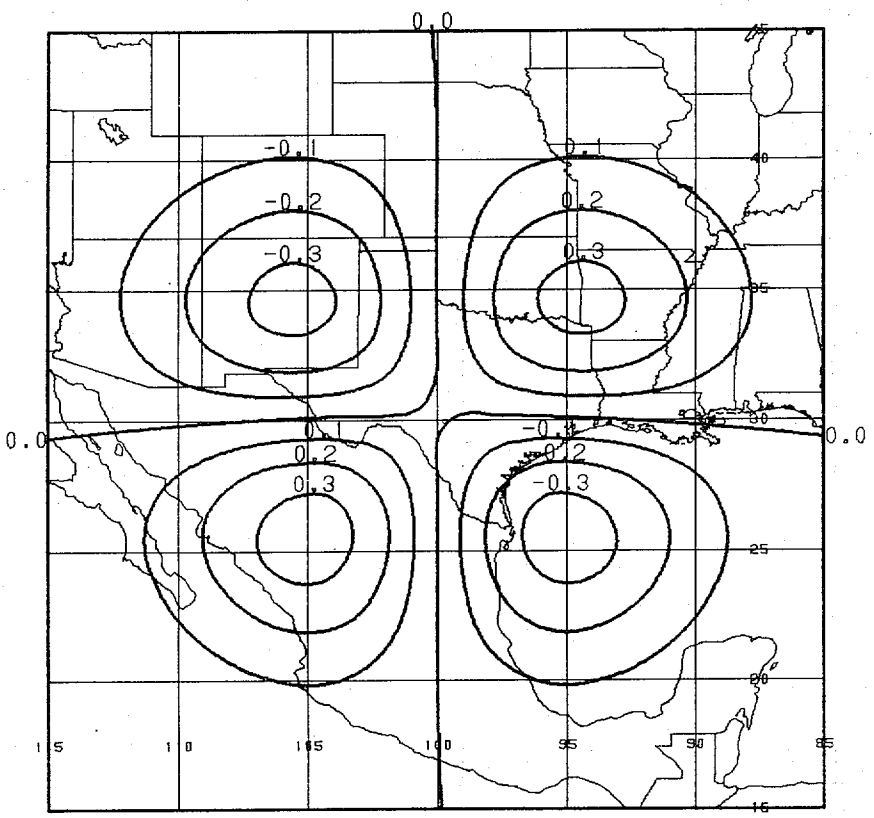


(b)

Figure 3. The (a) uz, (b) uv, (c) uu and (d) vv forecast error correlations centered at 30°N and 100°W for the case in which gradients of $\sigma^z$ are neglected.

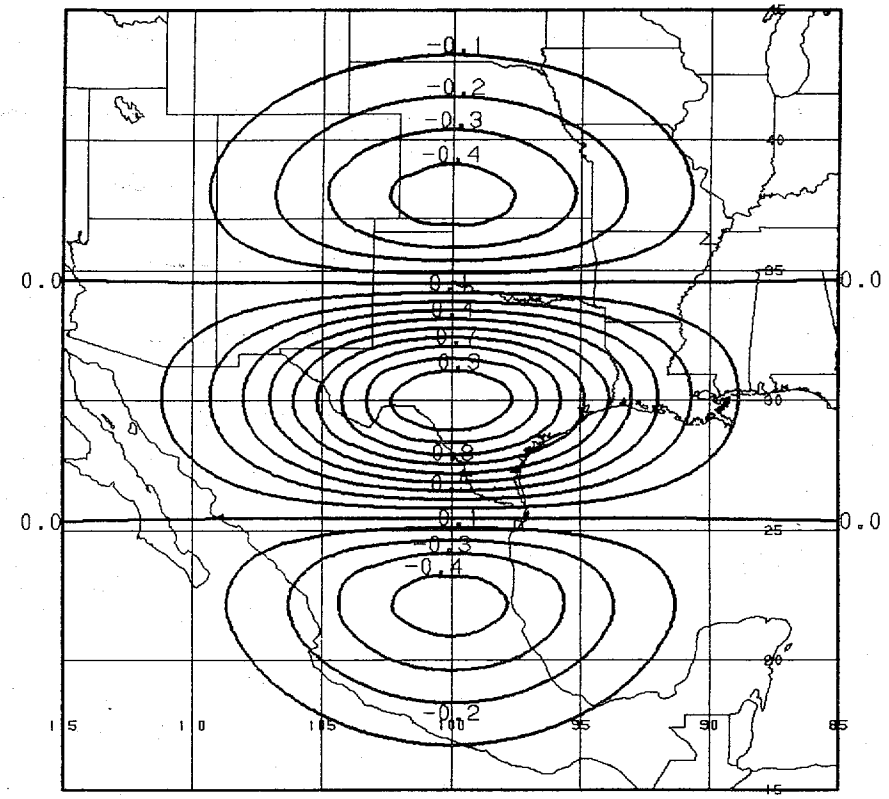
-0.1
-0.2
-0.3
-0.4
0.0
0.1
0.3
0.5
0.7
0.9
0.8
0.6
0.4
0.2
-0.2
0.0
0.0
0.0
115
110
105
100
95
90
85
45
40
35
30
25
20
15

(c)

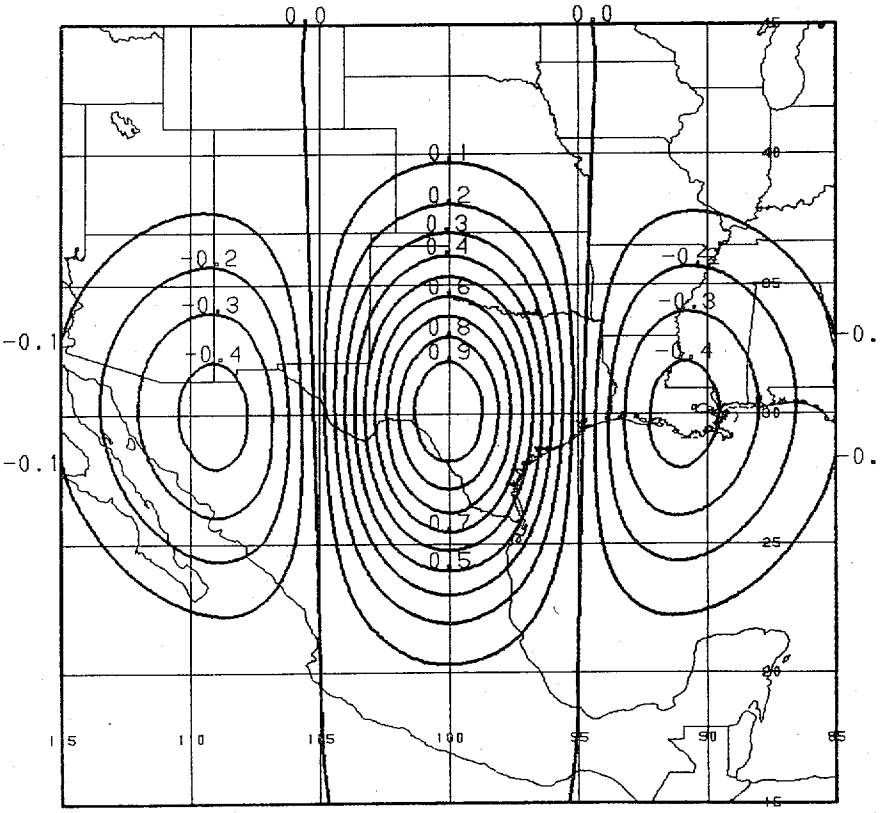
0.0
0.0
0.1
0.2
0.3
0.4
0.6
0.8
0.9
0.7
0.5
-0.2
-0.3
-0.4
-0.1
-0.1
0.1
0.1
115
110
105
100
95
90
85
45
40
35
30
25
20
15

(d)

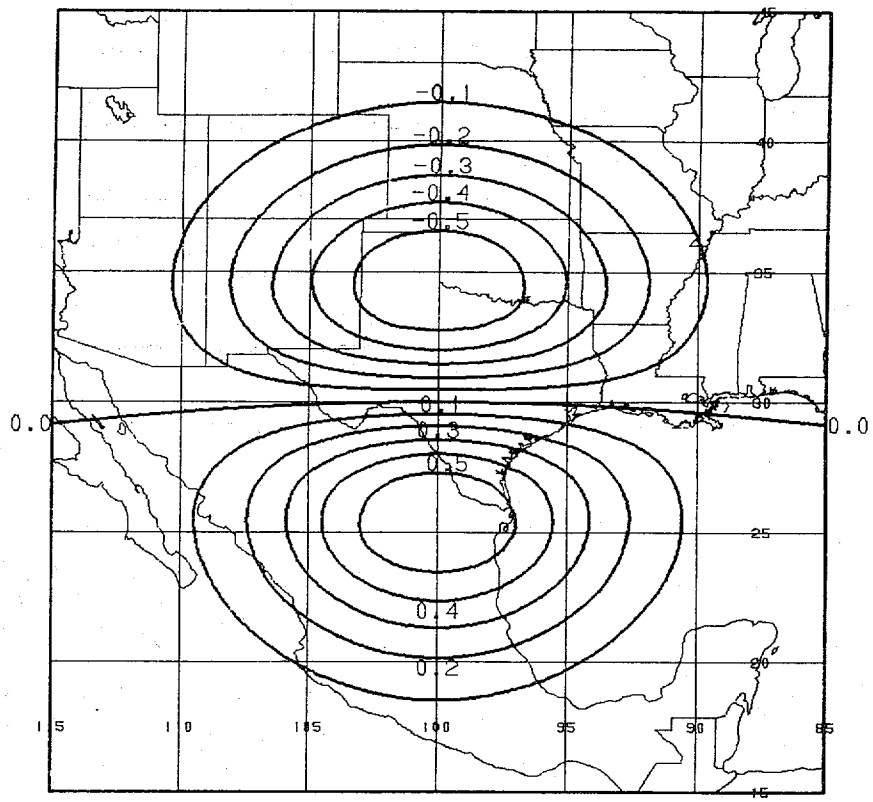


(a)

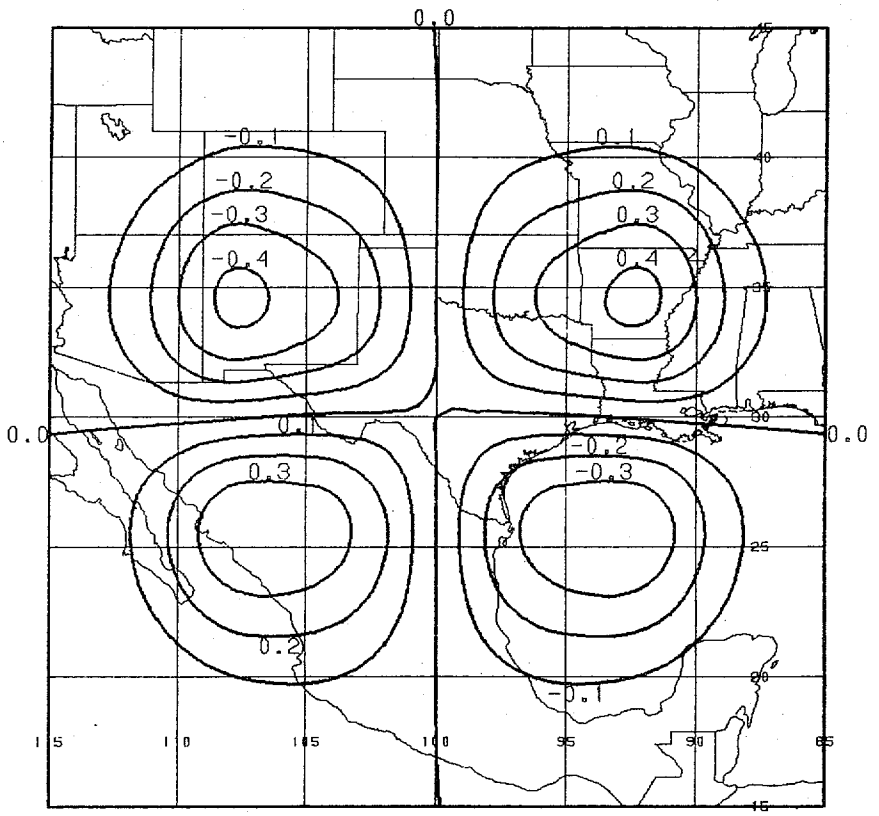


(b)

Figure 4. The (a) uz, (b) uv, (c) uu and (d) vv forecast error correlations for which the effect of the $\sigma^z$ field shown in Figure 2a is included.

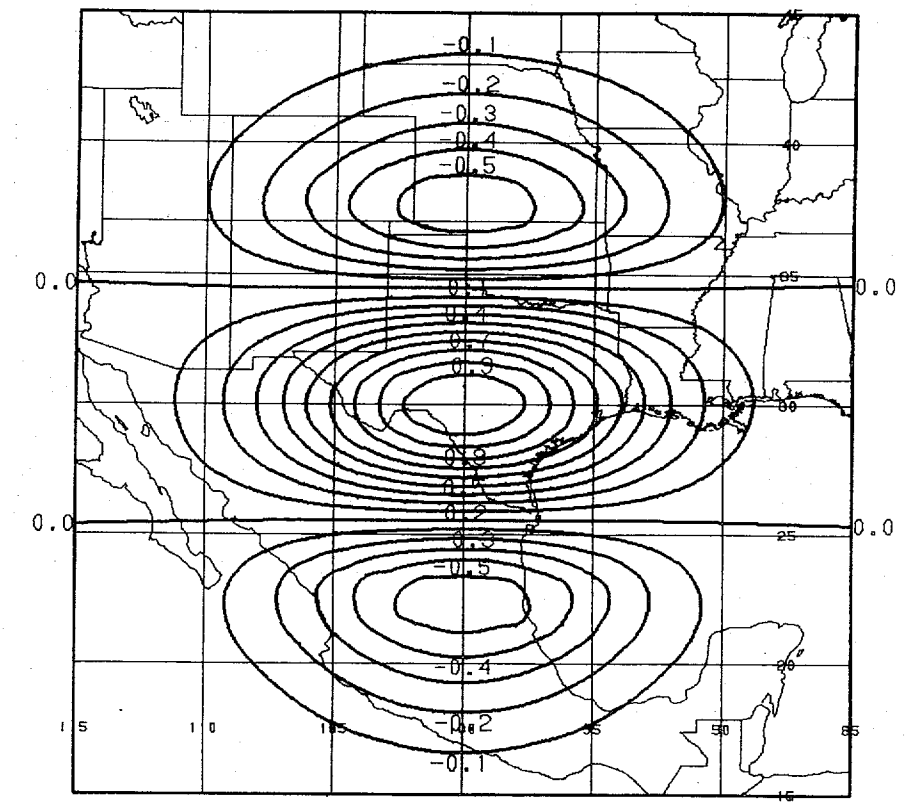
-0.1
-0.2
-0.3
-0.4
-0.5
0.0
0.1
0.2
0.3
0.4
0.5
0.6
0.7
0.8
0.9
0.0
0.0
-0.5
-0.4
-0.2
-0.1
115
110
105
35
50
85

(c)

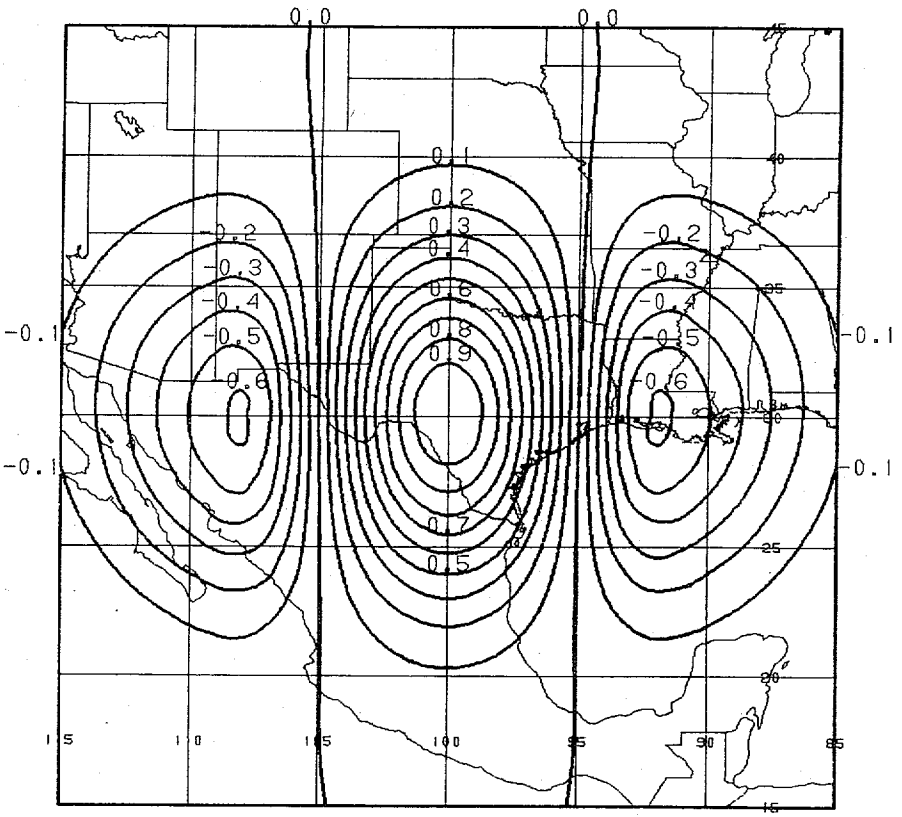
0.0
0.0
0.1
0.2
0.3
0.4
0.6
0.8
0.9
-0.2
-0.3
-0.4
-0.5
-0.6
-0.1
-0.1
0.7
0.5
115
110
105
100
95
90
85

(d)

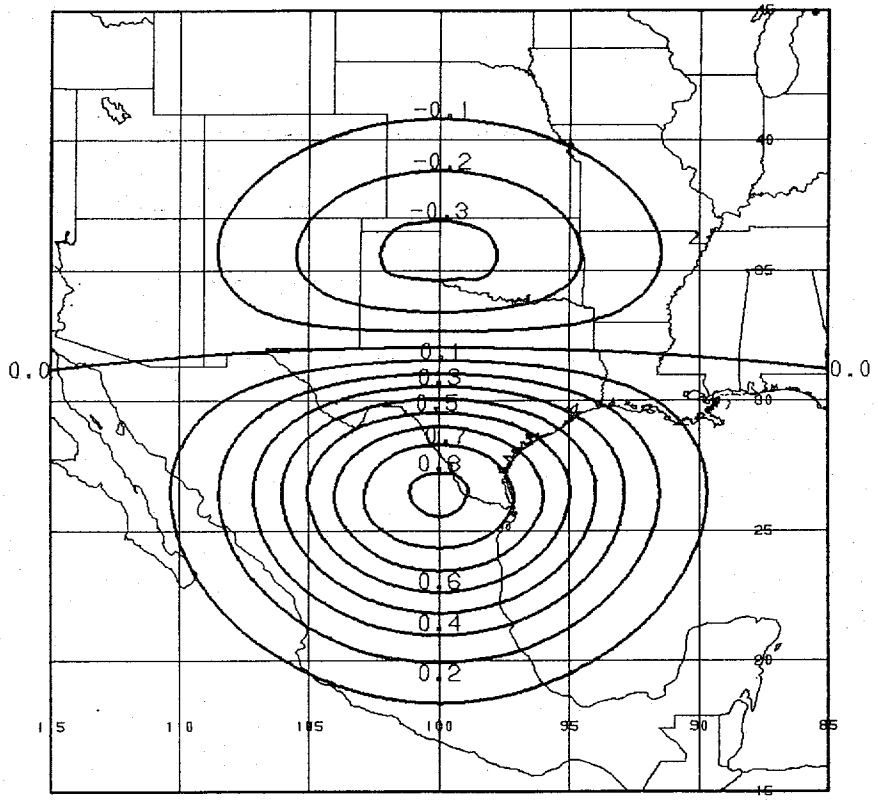


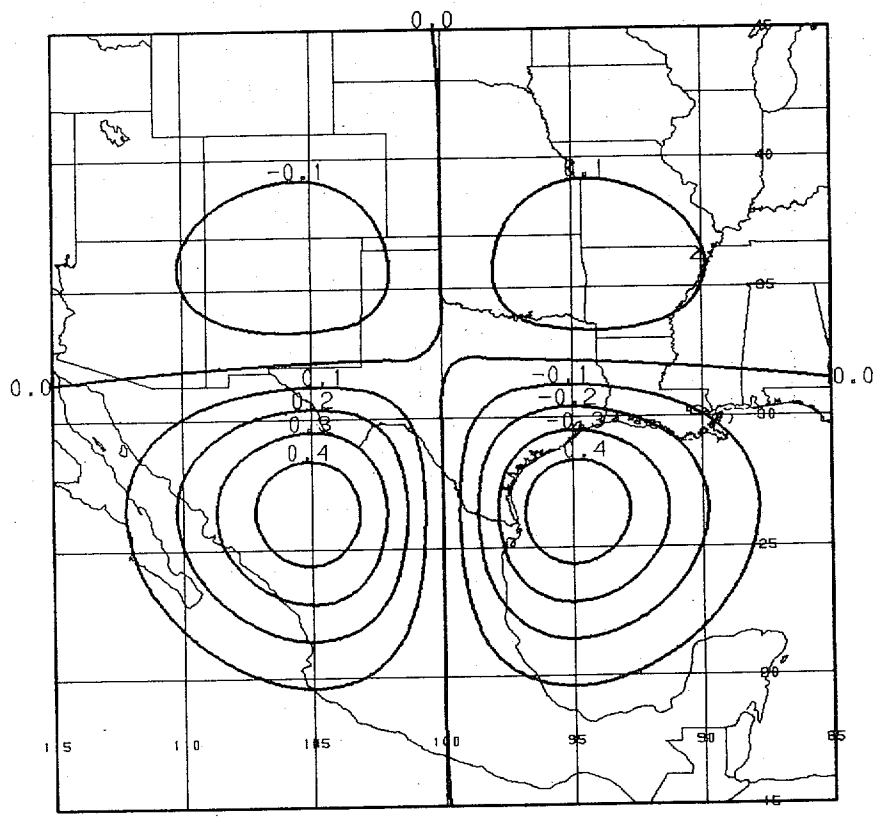


Figure 5. The (a) uz, (b) uv, (c) uu and (d) vv forecast error correlations for which the effect of the $\sigma^{z}$ field shown in Figure 2b is included.

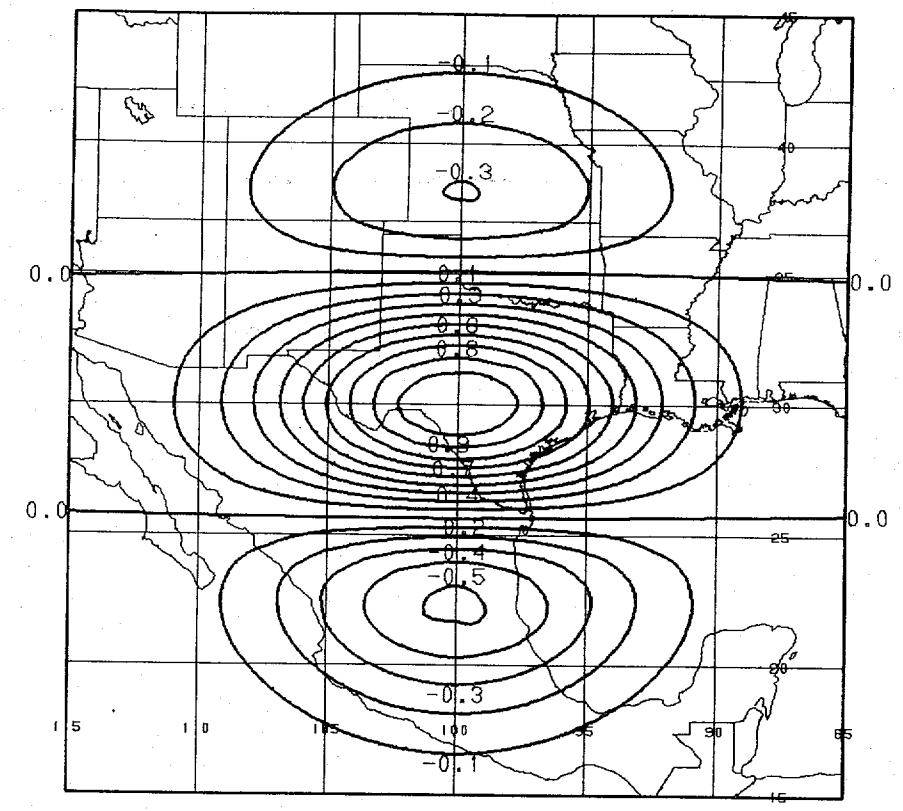
-0.1
-0.2
-0.3
0.0
0.1
0.5
0.6
0.8
0.9
0.4
0.2
-0.4
-0.5
-0.3
-0.1
0.0
0.0
45
40
35
30
25
20
15
115
110
105
100
95
90
85

(c)

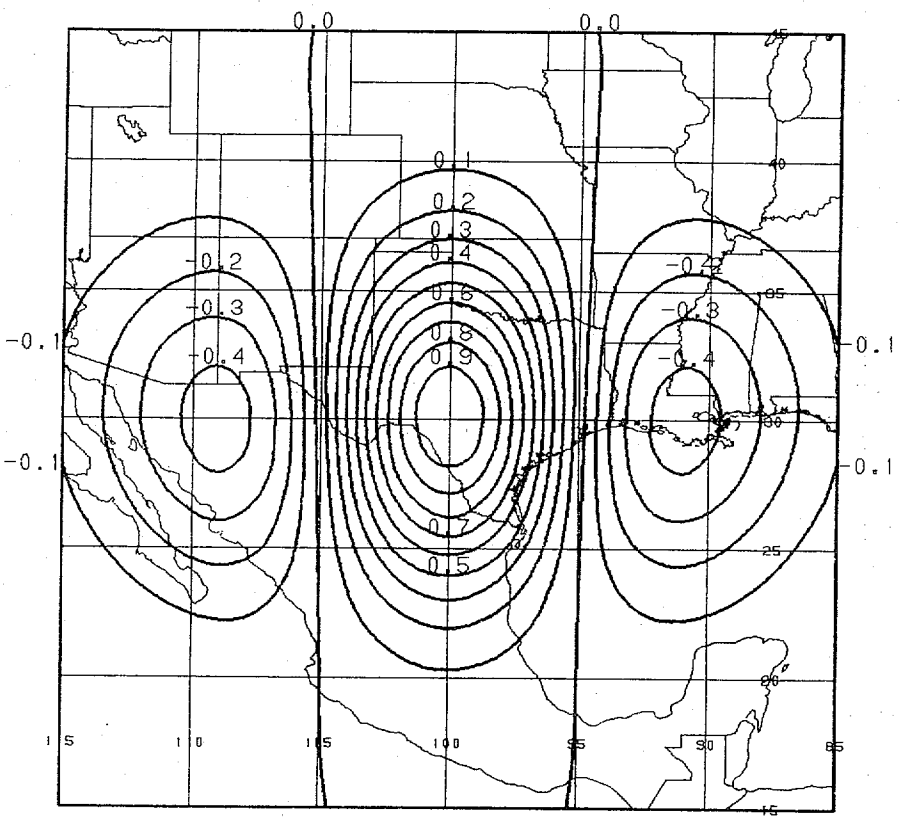
0.0
0.0
0.1
0.2
0.3
0.4
0.6
0.8
0.9
0.7
0.5
-0.2
-0.3
-0.4
-0.1
-0.1
45
40
35
30
25
20
15
115
110
105
100
95
90
85

(d)

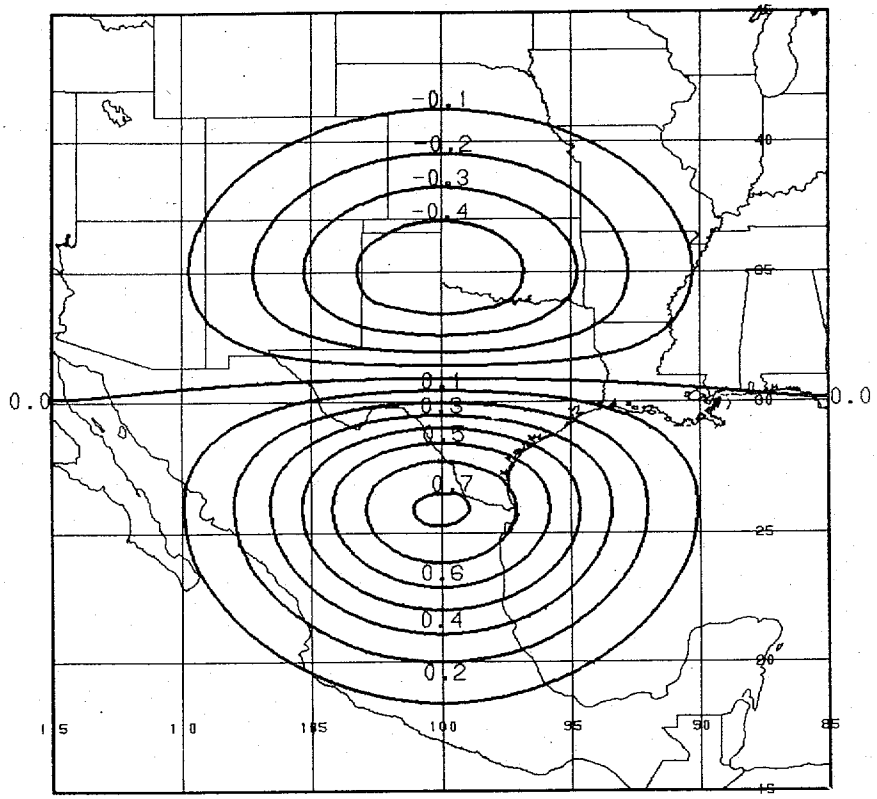


(a)

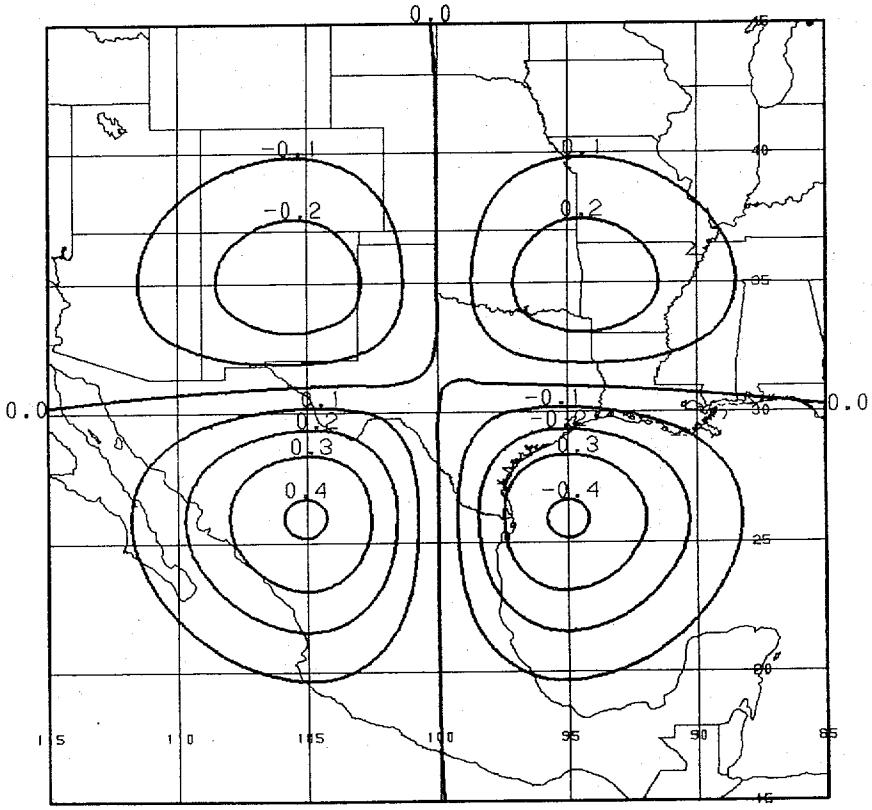


(b)

Figure 6. The (a) uz, (b) uv, (c) uu and (d) vv forecast error correlations for which the effect of the $\sigma^{\Sigma}$ field shown in Figure 2c is included.

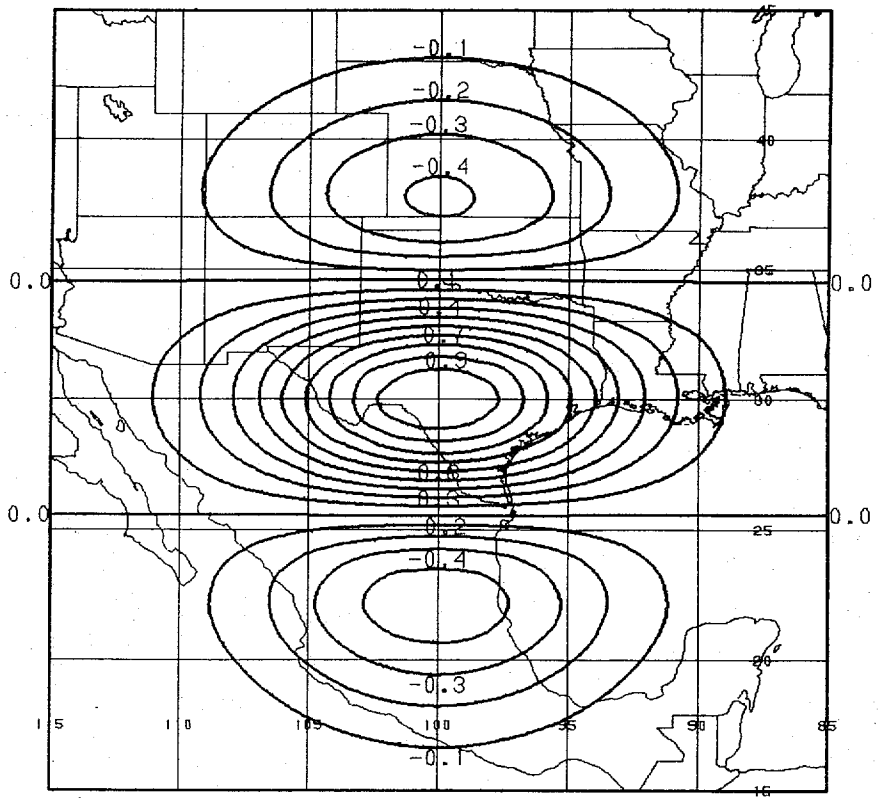
-0.1
-0.2
-0.3
-0.4
0.0
0.1
0.2
0.3
0.6
0.2
-0.4
-0.3
-0.1
0.0
0.0
0.0
45
40
35
30
25
20
15
115
110
105
100
95
90
85

(c)

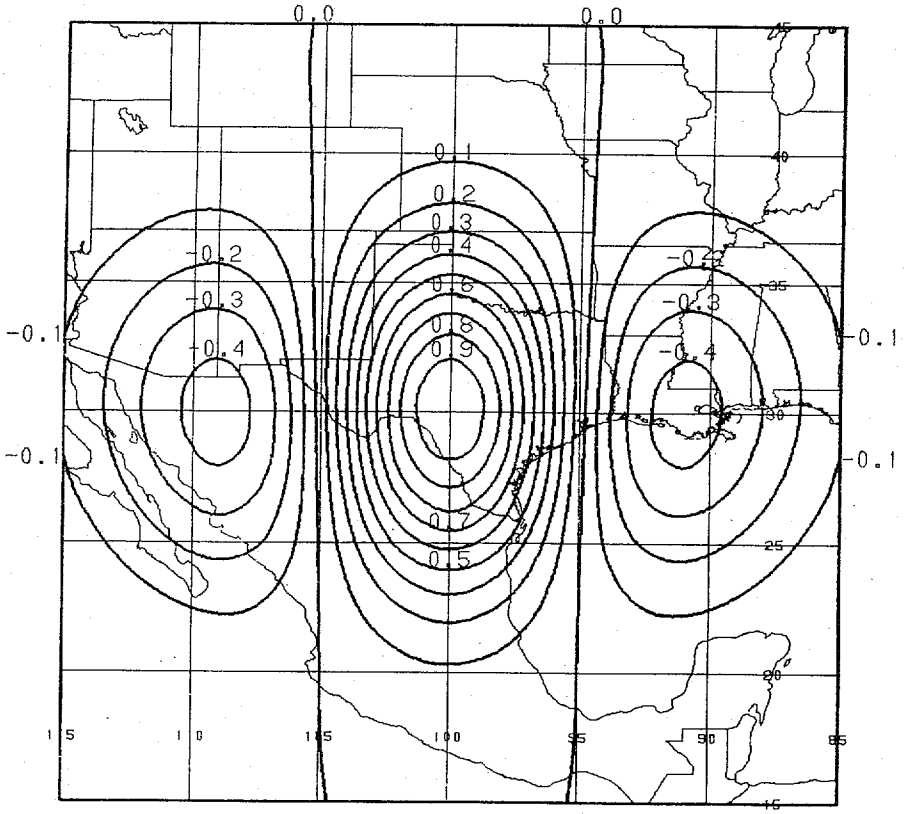
0.0
0.0
0.1
0.2
0.3
0.4
0.6
0.8
0.9
0.7
0.5
-0.2
-0.3
-0.4
-0.1
-0.1
-0.1
-0.1
45
40
35
30
25
20
15
115
110
105
100
95
90
85

(d)